INFECTION AND IMMUNITY, July 2008, p. 3346–3356 Vol. 76, No. 7
0019-9567/08/$08.00+0 doi:10.1128/IAI.00340-08

Molecular Variations in *Klebsiella pneumoniae* and *Escherichia coli* FimH Affect Function and Pathogenesis in the Urinary Tract[▽]

David A. Rosen, Jerome S. Pinkner, Jennifer N. Walker, Jennifer Stine Elam, Jennifer M. Jones, and Scott J. Hultgren*

Department of Molecular Microbiology, Washington University School of Medicine, St. Louis, Missouri 63110

Received 14 March 2008/Returned for modification 17 April 2008/Accepted 29 April 2008

Type 1 pili mediate binding, invasion, and biofilm formation of uropathogenic *Escherichia coli* (UPEC) in the host urothelium during urinary tract infection (UTI) via the adhesin FimH. In this study, we characterized the molecular basis of functional differences between FimH of the UPEC isolate UTI89 and the *Klebsiella pneumoniae* cystitis isolate TOP52. Type 1 pili characteristically mediate mannose-sensitive hemagglutination of guinea pig erythrocytes. Although the adhesin domain of *K. pneumoniae* TOP52 FimH ($FimH_{52}$) is highly homologous to that of *E. coli*, with an identical mannose binding pocket and surrounding hydrophobic ridge, it lacks the ability to agglutinate guinea pig erythrocytes. In addition, FimH-dependent biofilm formation in *K. pneumoniae* is inhibited by heptyl mannose, but not methyl mannose, suggesting the need for contacts outside of the mannose binding pocket. The binding specificity differences observed for $FimH_{52}$ resulted in significant functional differences seen in the pathogenesis of *K. pneumoniae* UTI compared to *E. coli* UTI. Infections in a murine model of UTI demonstrated that although the *K. pneumoniae* strain TOP52 required $FimH_{52}$ for invasion and IBC formation in the bladder, $FimH_{52}$ was not essential for early colonization. This work reveals that a limited amount of sequence variation between the FimH of *E. coli* and *K. pneumoniae* results in significant differences in function and ability to colonize the urinary tract.

Bacterial adherence to host mucosal surfaces is often an important first step in the infection process. This is especially true in the case of urinary tract infections (UTIs) (59). It is estimated that half of all women will experience at least one UTI in their lifetime (49), the vast majority of which are caused by uropathogenic *Escherichia coli* (UPEC) and other *Enterobacteriaceae* (48). An essential step in UPEC infection of the bladder is adherence to the host urothelial surface via type 1 pili (2, 27, 29). Type 1 pili are assembled via the chaperone/usher pathway (3, 30, 53). They are adhesive hair-like fibers consisting of cylindrical pilus rods composed of FimA pilin subunits and small-tip fibrillae composed of FimF, FimG, and the adhesin FimH (6, 31). The FimH adhesin recognizes mannosylated uroplakins and β-1 and α-3 integrin receptors on the luminal surface of bladder urothelial cells (17, 29, 63). Binding of UPEC to host cells induces a cascade of signaling events that ultimately leads to bacterial internalization and the formation of biofilm-like intracellular bacterial communities (IBCs) (1, 17, 22, 32, 39, 43, 51). IBC formation is also dependent on type 1 pili (62). Ultimately bacteria disperse from this intracellular niche and progress to infect other urothelial cells.

Type 1 piliated bacteria have historically been characterized by their ability to agglutinate guinea pig red blood cells (RBCs) in a mannose-sensitive manner (14, 15, 52). This mannose-sensitive hemagglutination (MSHA) phenotype of *E. coli* expressing type 1 pili requires the FimH adhesin. FimH consists of two domains: an amino-terminal adhesin domain (AD; receptor binding domain) and a carboxy-terminal pilin domain (PD) (8, 29, 31). FimH recognizes mannosylated glycoproteins, including those present on the host urothelium through its AD. FimH-mediated adhesion can be inhibited by D-mannose or oligosaccharides containing terminal mannose residues (5, 19–21). Additionally, it has been demonstrated that the FimH AD binds more tightly to α-D-mannosides with longer alkyl chains. Heptyl mannose was found to have the highest affinity for FimH (5). In animal models, neutralization of the adhesin by FimH-specific antibodies protects from UPEC cystitis (35, 36). X-ray crystal structures of FimH reveal a highly conserved mannose binding pocket at the tip of the FimH AD surrounded by a distal hydrophobic ridge (8, 29). Minor sequence differences in *E. coli* FimH, many of which are not located in close proximity to the mannose binding pocket, have been found to correlate with differential binding phenotypes (54–56).

Klebsiella pneumoniae is the second leading cause of gram-negative UTI but is a much less prevalent etiologic agent than UPEC. *K. pneumoniae* genes encode numerous chaperone/usher pili, including type 1 pili and type 3 pili (23). While type 1 pili have historically been defined by their MSHA phenotype, type 3 pili display a mannose-resistant hemagglutination (MRHA) with tannin-treated RBCs (47). Type 1 pili of *K. pneumoniae* are highly homologous to those of UPEC (23) and have been previously implicated in UTI pathogenesis (18, 40). The *fim* operon of *K. pneumoniae*, encoding type 1 pili, contains a terminal *fimK* gene, not present in UPEC, which plays a role in suppressing the expression of type 1 pili (50). *K. pneumoniae* binds, invades, and forms IBCs within host urothelial cells, albeit less efficiently than UPEC in the murine cystitis model. Similar to UPEC, *K. pneumoniae* also expresses type 1 pili within these IBCs (50). In this study, we discovered that type 1-piliated *K. pneumoniae* cells are unable to mediate hem-

* Corresponding author. Mailing address: Department of Molecular Microbiology and Microbial Pathogenesis, Box 8230, Washington University School of Medicine, 660 S. Euclid Ave., St. Louis, MO 63110. Phone: (314) 362-6772. Fax: (314) 362-1998. E-mail: hultgren@borcim.wustl.edu.

▽ Published ahead of print on 12 May 2008.

TABLE 1. Bacterial strains and plasmids used in this study

Strain or plasmid	Description	Reference
Strains		
UTI89	UPEC cystitis isolate	43
UTI89 Δ*fimH*	Knockout of *fimH* in UTI89	This study
TOP52 1721	*K. pneumoniae* cystitis isolate	50
TOP52 Δ*fimH*	Knockout of *fimH* in TOP52 1721	This study
TOP52 Δ*fimK*	Knockout of *fimK* in TOP52 1721	50
Plasmids		
pBAD33	Empty expression vector; P_{ara} Cm^r	24
p*fimX*	$fimX_{UTI89}$ expression vector; P_{ara} Cm^r	25
p$fimH_{89}$ (p*fimH*-$AD_{89}PD_{89}$)	$fimH_{UTI89}$ expression vector; P_{ara} Cm^r	This study
p*fimH*-$AD_{89}PD_{52}$	*fimH* chimera expression vector; P_{ara} Cm^r	This study
p*fimH*-$AD_{52}PD_{89}$	*fimH* chimera expression vector; P_{ara} Cm^r	This study
p$fimH_{52}$ (p*fimH*-$AD_{52}PD_{52}$)	$fimH_{TOP52}$ expression vector; P_{ara} Cm^r	This study

agglutination of guinea pig erythrocytes despite the presence of wild-type FimH containing an identical mannose binding pocket to *E. coli* FimH. We analyzed functional and structural differences in FimH of the *K. pneumoniae* strain TOP52 and the effects of these differences on UTI pathogenesis.

MATERIALS AND METHODS

Bacterial strains and culture conditions. A complete list of bacterial strains and plasmids used in this study can be found in Table 1. The clinical strains used include UTI89, a UPEC cystitis isolate (43), and TOP52 1721 (abbreviated TOP52 in this article), a *K. pneumoniae* cystitis isolate (50). Bacteria were cultured at 37°C in Luria-Bertani (LB) broth containing, as appropriate, 20 μg/ml chloramphenicol and 0.4% arabinose as indicated.

***K. pneumoniae* TOP52 and *E. coli* UTI89 mutant construction and complementation.** A targeted deletion of *fimH* in the *K. pneumoniae* isolate TOP52 was constructed with the pKOV vector as described previously (37). Flanking sequences of approximately 1,000 bp on each side of the targeted gene were amplified with the indicated primers (Table 2) and cloned into pKOV. Potential knockouts were screened by PCR, and the knockout region was sequenced. Growth curves were performed for mutant strains and showed no differences in growth compared to the wild type.

UTI89 Δ*fimH* was constructed using the red recombinase method as previously described (10, 44), with pKD4 as a template and the primers indicated (Table 2) followed by expression of the FLP recombinase to eliminate the kanamycin cassette. PCR using flanking primers was used to confirm the deletion.

For complementation studies, the ADs and PDs of both UTI89 *fimH* and TOP52 *fimH* were amplified using the primers indicated (Table 2). Subscripts 89 and 52 were used to indicate a given domain was from UTI89 or TOP52, respectively. Single ADs and PDs were added together as templates in a PCR to create a full-length *fimH* gene that was subsequently cloned into the arabinose-inducible pBAD33 vector (abbreviated pBAD). The four permutations of the ADs and PDs yielded *fimH* complementation vectors $pAD_{89}PD_{89}$ (p$fimH_{89}$), $pAD_{89}PD_{52}$, $pAD_{52}PD_{89}$, and $pAD_{52}PD_{52}$ (p$fimH_{52}$). All constructs were verified and sequenced using pBAD plasmid primers.

HAs. Hemagglutination assays (HAs) were performed with guinea pig RBCs (optical density at 640 nm [OD_{640}] of 2.0; Colorado Serum Company) as previously described using serial dilutions in microtiter plates with and without the addition of 100 mM methyl α-D-mannopyranoside (28).

Biofilm assays. Bacteria were grown in LB broth in wells of microtiter plates in the presence of 0.01% arabinose and either no mannose, 1 mM methyl mannose, 100 mM methyl mannose, or 1 mM heptyl mannose. After 48 h of growth at room temperature, wells were rinsed and then stained with crystal violet, and biofilms were quantified as previously described (46).

Modeling of *K. pneumoniae* FimH. *K. pneumoniae* TOP52 FimH was modeled onto the X-ray crystal structure of *E. coli* FimH from the J96 isolate FimC-H complex structure (PDB identification 1KLF) (29) using the protein structure threading program Phyre (4). The resulting model was compared to the J96

TABLE 2. Primer sequences

Name	Use	Sequence
NotIFimHF1	Amplify 1-kb *K. pneumoniae fimH* 5′ flanking region	5′-CGGTAACGCGGCCGCGGCGAATCGAAGGATTTTACT-3′
BamHIFimHR2	Amplify 1-kb *K. pneumoniae fimH* 5′ flanking region	5′-AACGGATCCAAAGGACCAGGCGTTCATC-3′
BamHIFimHF3	Amplify 1-kb *K. pneumoniae fimH* 3′ flanking region	5′-AACGGATCCACGCGATCTTCACCAATACC-3′
SalIFimHR4	Amplify 1-kb *K. pneumoniae fimH* 3′ flanking region	5′-AACGTCGACGTCTGGGGGTGAAGTACCTG-3′
FimHCheckF1	Check TOP52 Δ*fimH*	5′-GGACAGCACCGGCTATTACA-3′
FimHCheckR2	Check TOP52 Δ*fimH*	5′-GGGATCGTCAGGGAGATACA-3′
UTI89fimH KO F	Knock out *fimH* in *E. coli* UTI89	5′-ATGAAACGAGTTATTACCCTGTTTGCTGTACTGCTGATGGGCTGGTCGGTAGTGTAGGCTGGAGCTGCTTC-3′
UTI89fimH KO R	Knock out *fimH* in *E. coli* UTI89	5′-TTATTGATAAACAAAAGTCACGCCAATAATCGATTGCACATTCCCTGCAGTCATATGAATATCCTCCTTAG-3′
UTI89fimHcheckF	Check UTI89 Δ*fimH*	5′-CAATCAGCGCACTTCCCGTTACAGG-3′
UTI89fimHcheckR	Check UTI89 Δ*fimH*	5′-CTCGAATTATAAACAACCCGCGGCG-3′
2KlebphaseF	Amplify *fimS* region for phase assay	5′-GGGACAGATACGCGTTTGAT-3′
2KlebphaseR	Amplify *fimS* region for phase assay	5′-GGGACAGATACGCGTTTGAT-3′
ADecoliF	Amplify *E. coli fimH* adhesin domain	5′-AATTCCATGGGATGAAACGAGTTATTACCCTGTTTGCTG-3′
ADecoliR	Amplify *E. coli fimH* adhesin domain	5′-TCGCAGCCGCCAGTGGGCACCACCAC-3′
PDecoliF	Amplify *E. coli fimH* pilin domain	5′-GTGGTGGTGCCCACTGGCGGCTGCGA-3′
PDecoliR	Amplify *E. coli fimH* pilin domain	5′-AATTGGTACCATTGATAAACAAAAGTCACGCCAATAATCG-3′
ADklebF	Amplify *K. pneumoniae fimH* adhesin domain	5′-AATTCCATGGGATGATGAAAAAAATAATCCCCCTGTTCACC-3′
ADklebR	Amplify *K. pneumoniae fimH* adhesin domain	5′-TCGCAGCCGCCGGTGGGGACCACCAC-3′
PDklebF	Amplify *K. pneumoniae fimH* pilin domain	5′-GTGGTGGTCCCCACCGGCGGCTGCGA-3′
PDklebR	Amplify *K. pneumoniae fimH* pilin domain	5′-AATTGGTACCCATTGATAGACAAAGGTGATGCCGATG-3′
pBADF	Check pBAD33 clones	5′-TATCGCAACTCTCTACTGTTTCTCCA-3′
pBADR	Check pBAD33 clones	5′-CTGTATCAGGCTGAAAATCTTCTCTCA-3′

structure and UTI89 amino acid sequence. (A structure for UTI89 FimH has not been solved to date, and J96 FimH differs by only 4 amino acids [aa] from UTI89 FimH.) Figures were rendered in the molecular modeling program Pymol (11).

Mouse infections. Bacterial strains were used to inoculate 8-week-old female C3H/HeN mice (National Cancer Institute) by transurethral catheterization as previously described (42). Twenty-five-milliliter static cultures were inoculated from freezer stocks and grown at 37°C for 18 h and then subcultured 1:250 into 25 ml fresh medium. These cultures were then grown statically at 37°C for 18 h and centrifuged for 5 min at 5,800 rpm, and the resultant pellet was resuspended in phosphate-buffered saline (PBS) and diluted to approximately 2×10^8 CFU/ml. Fifty microliters of this suspension was used to infect each mouse with an inoculum of 1×10^7 to 2×10^7 CFU. All studies were approved by the Animal Studies Committee at Washington University School of Medicine.

Organ titers, gentamicin protection assays, and IBC enumeration. To quantify bacteria present in mouse organs, bladders and kidneys were aseptically harvested at the indicated times postinfection, homogenized in PBS, serially diluted, and plated onto LB agar plates. Luminal and intracellular bacteria were quantified using an ex vivo gentamicin protection assay as previously described (33). For ex vivo enumeration of IBCs, infected bladders were harvested at 1 h postinfection, bisected, splayed, washed with PBS, fixed with 3% paraformaldehyde for 1 h at room temperature and *lacZ* stained as previously described (33). IBCs were visualized and counted using an Olympus SZX12 dissecting microscope (Olympus America).

***fim* operon phase assay.** To determine the orientation of the type 1 pilus phase-variable promoter switch (*fimS*) in UTI89 Δ*fimH*, a phase assay was performed as previously described (58). Briefly, PCR primers were used to amplify a 589-bp DNA region including *fimS*. The PCR product was then digested with the restriction endonuclease HinfI (New England Biolabs) and was separated on a 2.5% agarose gel. A phase-on switch results in products of 489 and 70 bp and a phase-off switch results in products of 359 and 200 bp.

Immunoelectron microscopy. Bacteria were prepared as described above for mouse infection, fixed with 1% paraformaldehyde for 10 min, and absorbed onto Formvar/carbon-coated copper grids for 2 min. Grids were washed two times with PBS, blocked with 1% fetal bovine serum for 5 min, and incubated with rabbit anti-FimH antibody (1:100) for 30 min at room temperature. The rabbit anti-FimH antibody was raised against the FimH adhesin domain (positions 1 to 159, T2) of *E. coli* J96 (26) (SigmaGenesis). Grids were subsequently washed two times with PBS, blocked with 1% fetal bovine serum for 5 min, and incubated with 18-nm colloidal gold particle-conjugated anti-rabbit immunoglobulin G (Jackson ImmunoResearch Laboratories) for 30 min at room temperature. Following two PBS washes, grids were rinsed in distilled water and stained with 1% aqueous uranyl acetate (Ted Pella, Inc.) for 1 min. Excess liquid was gently wicked off, and grids were air dried. Samples were viewed on a JEOL 1200EX transmission electron microscope (JEOL USA) at 80 kV accelerating voltage.

Statistical analysis. Continuous variables were compared using the Mann-Whitney U test since these variables were not normally distributed. All tests were two-tailed, and a P value of <0.05 was considered significant. Analyses were performed using GraphPad Prism (version 4.03) and SAS (version 9.0).

Nucleotide sequence accession number. The TOP52 *fimH* nucleotide sequence has been deposited in the GenBank database under accession no. EU327536.

RESULTS

Type 1-piliated *K. pneumoniae* TOP52 is hemagglutination negative. In contrast to UPEC, statically passaged *K. pneumoniae* TOP52 produced no detectable hemagglutination of guinea pig RBCs despite expression of type 1 pili (Table 3). The MSHA titer of the UPEC strain UTI89 was 1:512. Deletion of *fimH* abolished the ability of UTI89 Δ*fimH* to produce MSHA. UTI89 Δ*fimH* produced a low MRHA titer of 1:4, unlike UTI89. Wild-type *K. pneumoniae* TOP52 did not agglutinate guinea pig erythrocytes. Deletion of *fimH* to create TOP52 Δ*fimH* was also negative for hemagglutination. Recently, we discovered that deletion of *fimK*, a gene unique to *Klebsiella fim* gene clusters, resulted in a hyper-type 1-piliated phenotype (50). The hyperpiliated TOP52 Δ*fimK* was also hemagglutination negative. The *fimX* recombinase has been shown to have *fimB*-like properties (7, 25), and its overexpression results in increased expression of type 1 pili in both *E. coli* (25) and *K. pneumoniae* (50). The hyperpiliated TOP52/p*fimX* was also hemagglutination negative. Thus, type 1-piliated *K. pneumoniae* TOP52 is unable to mediate MSHA.

TABLE 3. $FimH_{52}$-specific inability of *K. pneumoniae* TOP52 to agglutinate guinea pig RBCs

Strain	HA titer ($1:2^x$) in guinea pig RBCs[a]:	
	Without mannose	With mannose
UTI89	9	2
UTI89 Δ*fimH*	2	2
TOP52	0	0
TOP52 Δ*fimH*	0	0
TOP52 Δ*fimK*	0	0
TOP52/pBAD	0	0
TOP52/p*fimX*	0	0
TOP52 Δ*fimH*/pBAD	0	0
TOP52 Δ*fimH*/p$fimH_{52}$	0	0
TOP52 Δ*fimH*/p$fimH_{89}$	4	0

[a] HA titer data are representative of three independent experiments.

$FimH_{52}$ and $FimH_{89}$ are highly similar in amino acid sequence and predicted structure. To further investigate the functional differences of *K. pneumoniae* TOP52 type 1 pili, we sequenced $fimH_{52}$ (GenBank accession no. EU327536) and compared it to other known *K. pneumoniae* FimH sequences and the sequence of *E. coli* UTI89 FimH ($FimH_{89}$). The $FimH_{52}$ amino acid sequence shares 100% identity with the FimH adhesin domain of *K. pneumoniae* strain IA565 (23), 99.6% amino acid identity with the FimH of *K. pneumoniae* ATCC 700721 strain (41), and 85.3% amino acid identity with *K. pneumoniae* strain IA551 (16). $FimH_{52}$ has 86.4% amino acid identity to FimH of *E. coli* UTI89 ($FimH_{89}$) (Fig. 1A) and maintains the general bidomain composition of *E. coli* FimH with an amino-terminal adhesin domain (amino acids [aa] 1 to 157) and a carboxy-terminal pilin domain (aa 161 to 279) separated by a short linker region.

We threaded *K. pneumoniae* FimH onto the X-ray crystal structure of FimH from the complex structure of FimC-H from the J96 *E. coli* isolate (29). We then overlaid J96 FimH and TOP52 FimH and compared the positions and identities of amino acid differences in $FimH_{89}$ and $FimH_{52}$ (Fig. 1B). This comparison assumes that residues conserved between J96 FimH and UTI89 FimH have the same conformation as shown in the three-dimensional J96 FimH structure. There are only four amino acid differences between FimH of these two strains. Seventeen AD amino acid differences and 21 PD amino acid differences exist between $FimH_{89}$ and $FimH_{52}$. Interestingly, $FimH_{52}$ displays full conservation of the residues known to interact with mannose in the mannose binding pocket (orange) and those that form the surrounding hydrophobic ridge (green in Fig. 1). Residue differences exist in areas adjacent to the receptor binding site and in other more distal parts of the molecule, which may together alter the molecular details of the interaction with mannose. Two differences in $FimH_{52}$ primary sequence exist in residues adjacent to known mannose-binding residues (His132 and Ser141, changed from Arg and Asp, respectively, in $FimH_{89}$). The threaded model $FimH_{52}$ suggests that these residues would lie ~8.5 Å away from the bound mannose moiety. Arg132 and Asp141 form a salt bridge in *E. coli* FimH that helps stabilize the structure of the FG

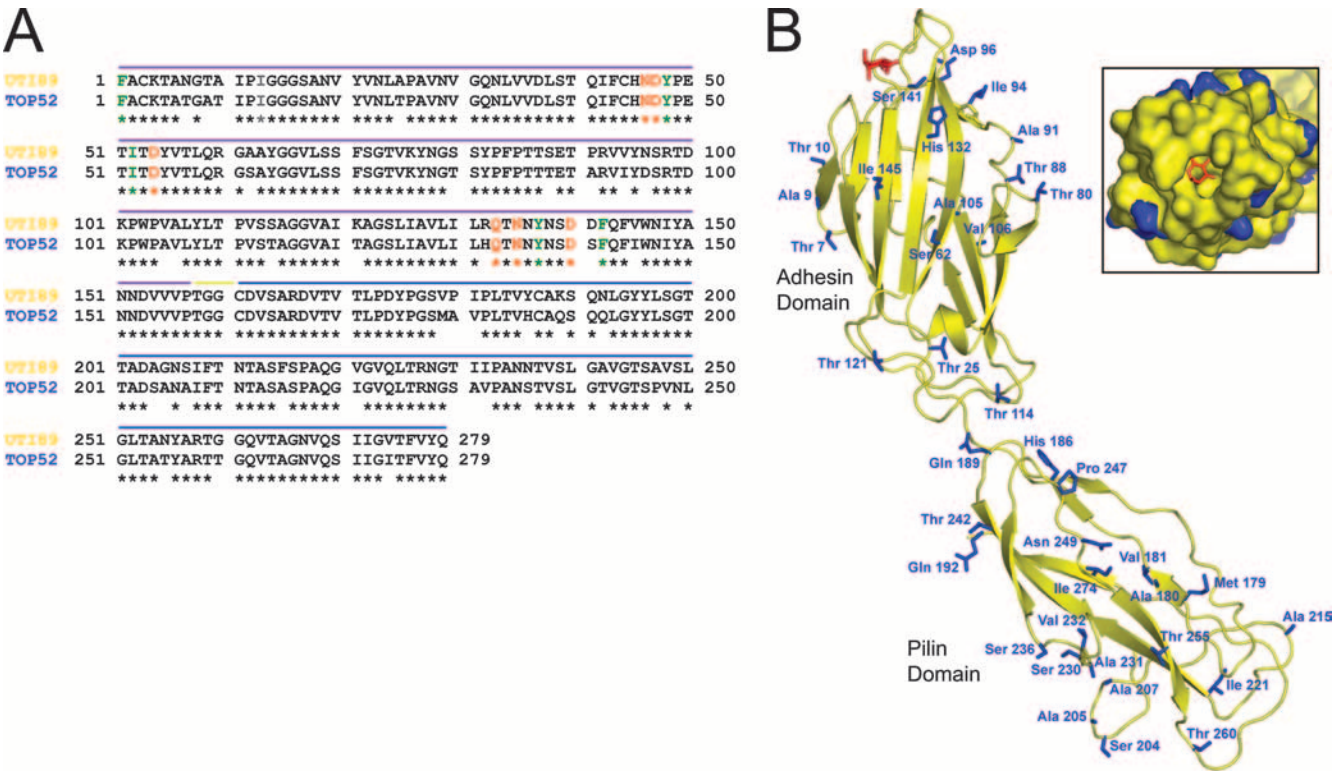

FIG. 1. $FimH_{52}$ and $FimH_{89}$ are highly conserved in sequence and structure. (A) The FimH amino acid sequences of *E. coli* UTI89 and *K. pneumoniae* TOP52 are shown. Residues known to interact with mannose (orange) and form the hydrophobic ridge (green) are fully conserved. The purple line denotes sequence of the AD, the blue line denotes sequence of the PD, and the yellow line denotes the short linker region. Amino acid numbers refer to the mature protein without signal sequence. (B) Structure of *E. coli* FimH (yellow) (from the J96 strain FimC-H complex; PDB identification no. 1KLF) bound to mannose (red) overlaid with a threaded model of *K. pneumoniae* TOP52 FimH. Side chains of TOP52 amino acids that vary from the UTI89 sequence are shown as blue sticks. (Inset) Space-filling model of a view into the mannose binding pocket (same colors described above). This shows that all residues in direct contact with the mannose moiety and those that form the hydrophobic ridge are fully conserved between *E. coli* UTI89 and *K. pneumoniae* TOP52.

loop that contains mannose binding residues Gln133, Asn135, and Asp140 and forms part of the hydrophobic ridge. Arg132 NH1 also makes two hydrogen bonds to Gln59 OE1 and Glu89 OE1. In $FimH_{52}$, His132 is only able to make a single hydrogen bond with Glu89 OE2. Differences in these and other residues may help explain the inability of *K. pneumoniae* TOP52 to agglutinate guinea pig RBCs.

The inability of *K. pneumoniae* TOP52 to agglutinate guinea pig RBCs is specific to the adhesin domain of $FimH_{52}$. Although all residues involved in direct interactions with the mannose moiety and all those in the surrounding hydrophobic ridge are identical between $FimH_{52}$ and $FimH_{89}$, nearly 14% of amino acids differ between the two proteins. We hypothesized that if this variation in FimH sequence accounts for the inability to agglutinate guinea pig erythrocytes, then complementation of TOP52 Δ*fimH* with *fimH* cloned from *E. coli* UTI89 ($fimH_{89}$), should restore the MSHA phenotype. Thus, TOP52 Δ*fimH* was complemented with the *fimH* gene of *K. pneumoniae* TOP52 ($fimH_{52}$) or $fimH_{89}$ on inducible plasmids. While the TOP52 Δ*fimH*/pBAD vector control and TOP52 Δ*fimH*/p$fimH_{52}$ were hemagglutination negative, TOP52 Δ*fimH*/p$fimH_{89}$ had an MSHA titer of 1:16 (Table 3). Thus, $FimH_{89}$ is able to participate in type 1 pilus biogenesis with the Fim proteins of *K. pneumoniae* TOP52 and confers a gain of MSHA function.

To test the expression of exogenous *fimH* in the UTI89 Δ*fimH* background, phase assays were conducted analyzing the phase-variable promoter switch of type 1 pili (Fig. 2). The *fim* operon of wild-type *E. coli* UTI89 was primarily phase on after static growth; however, loss of *fimH* in UTI89 Δ*fimH* and the UTI89 Δ*fimH*/pBAD vector control resulted in bacterial populations that were primarily in the phase-off orientation. Complementation with either p$fimH_{89}$ or p$fimH_{52}$ did not result in a robust off-to-on switch as the populations remained primarily phase off with similarly low levels of piliated bacteria. However, enough phase-on bacteria were present to detect an MSHA titer with p$fimH_{89}$ complementation (Table 3).

$FimH_{52}$ and $FimH_{89}$ function was investigated further by constructing FimH chimeras. We used the chimeras to complement *fimH*-knockout strains and then examined the final pilus assembly on each strain by immunoelectron microscopy. The ADs and PDs of each strain were amplified and expressed in different combinations on the arabinose-inducible pBAD33 vector. This resulted in four different *fimH* construct-expressing plasmids: $pAD_{89}PD_{89}$ (p$fimH_{89}$), $pAD_{89}PD_{52}$, $pAD_{52}PD_{89}$, and $pAD_{52}PD_{52}$ (p$fimH_{52}$).

The incorporation of p$fimH_{89}$, $pAD_{89}PD_{52}$, $pAD_{52}PD_{89}$, and p$fimH_{52}$ into pili was confirmed by immunoelectron microscopy using anti-FimH antibodies. Consistent with the

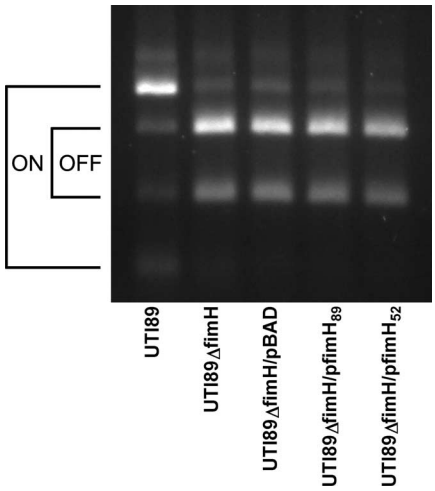

FIG. 2. The *fim* operon of UTI89 Δ*fimH* is primarily in the phase-off orientation. Phase assays of the *fimS* invertible promoter region of the *fim* operon were done for *E. coli* UTI89, UTI89 Δ*fimH*, UTI89 Δ*fimH*/pBAD, UTI89 Δ*fimH*/p*fimH*$_{89}$, and UTI89 Δ*fimH*/p*fimH*$_{52}$. UTI89 was largely phase on, while the UTI89 Δ*fimH* strains were all primarily phase off despite complementation.

TABLE 4. Adhesin domain-specific hemagglutination deficiency of *K. pneumoniae* TOP52 FimH$_{52}$

Strain	HA titer (1:2^x) in guinea pig RBCs[a]:	
	Without mannose	With mannose
UTI89	9	3
UTI89 Δ*fimH*	2	2
UTI89 Δ*fimH*/pBAD	0	0
UTI89 Δ*fimH*/pfimH$_{89}$	5	0
UTI89 Δ*fimH*/pAD$_{89}$PD$_{52}$	5	0
UTI89 Δ*fimH*/pAD$_{52}$PD$_{89}$	0	0
UTI89 Δ*fimH*/p*fimH*$_{52}$	0	0
TOP52	0	0
TOP52 Δ*fimH*	0	0
TOP52 Δ*fimH*/pBAD	0	0
TOP52 Δ*fimH*/p*fimH*$_{89}$	4	0
TOP52 Δ*fimH*/pAD$_{89}$PD$_{52}$	4	0
TOP52 Δ*fimH*/pAD$_{52}$PD$_{89}$	0	0
TOP52 Δ*fimH*/p*fimH*$_{52}$	0	0

[a] HA titer data are representative of three independent experiments.

phase switch being primarily off in these complementations, the majority of bacteria were bald without noticeable pili. However, similar subpopulations of bacteria existed in each sample that were moderately piliated and immunolabeling at the tips of pili was observed for UTI89 Δ*fimH* complemented with each construct (Fig. 3). The low level of type 1 pilus expression explains the inability to fully complement UTI89 Δ*fimH* to wild-type *E. coli* UTI89 MSHA titers.

TOP52 Δ*fimH* was also complemented with each FimH chimera and the MSHA titers for all strains were analyzed (Table 4). Wild-type UTI89 produced an MSHA titer of 1:512, while wild-type TOP52 was hemagglutination negative. UTI89 Δ*fimH*, UTI89 Δ*fimH*/pBAD, TOP52 Δ*fimH*, and TOP52 Δ*fimH*/pBAD all lacked the ability to agglutinate guinea pig RBCs. UTI89 Δ*fimH*/p*fimH*$_{89}$ and UTI89 Δ*fimH*/pAD$_{89}$PD$_{52}$ both produced an MSHA titer of 1:32, while UTI89 Δ*fimH*/pAD$_{52}$PD$_{89}$ and UTI89 Δ*fimH*/p*fimH*$_{52}$ did not produce a hemagglutination titer. This trend was recapitulated in the TOP52 Δ*fimH* background. While TOP52 Δ*fimH*/p*fimH*$_{52}$ and TOP52 Δ*fimH*/pAD$_{52}$PD$_{89}$ both lacked hemagglutination titers, TOP52 Δ*fimH*/p*fimH*$_{89}$ and TOP52 Δ*fimH*/pAD$_{89}$PD$_{52}$ both produced MSHA titers of 1:16.

These results demonstrate that the *K. pneumoniae* TOP52 FimH inability to agglutinate guinea pig RBCs is specific to its AD. The AD of *E. coli* UTI89 FimH is capable of agglutinating guinea pig RBCs with the native UTI89 PD or with the PD of *K. pneumoniae* TOP52. Thus, variations between the FimH ADs of *E. coli* UTI89 and *K. pneumoniae* TOP52 are likely responsible for their differences in function.

***K. pneumoniae* TOP52 FimH-dependent biofilms are inhibited by heptyl mannose but not methyl mannose.** *K. pneumoniae* TOP52 is able to form biofilm at room temperature when the production of type 1 pili is induced via the *E. coli* recombinase, coded for by *fimX* (50). Thus, we investigated whether this biofilm was FimH dependent. Biofilms were stained with crystal violet and quantified after 48 h of incubation. Wild-type TOP52 and TOP52/pBAD vector control did not form biofilm, while TOP52/p*fimX* formed biofilm. TOP52 Δ*fimH*, TOP52 Δ*fimH*/pBAD, and TOP52 Δ*fimH*/p*fimX* did not form biofilm, suggesting that the TOP52/p*fimX* biofilm is

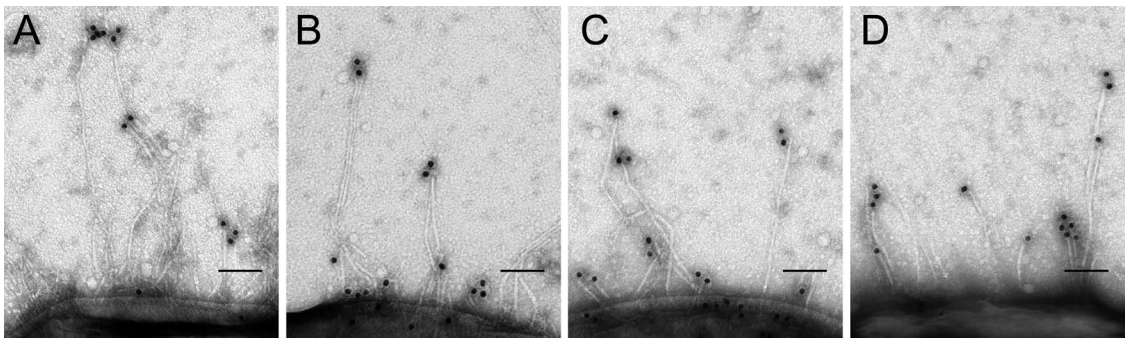

FIG. 3. *fimH* constructs in UTI89 Δ*fimH* are expressed in some bacteria and localized at the tips of pili. Immunoelectron microscopy using an anti-FimH antibody was performed against UTI89 Δ*fimH*/p*fimH*$_{89}$ (A), UTI89 Δ*fimH*/pAD$_{89}$PD$_{52}$ (B), UTI89 Δ*fimH*/pAD$_{52}$PD$_{89}$ (C), and UTI89 Δ*fimH*/p*fimH*$_{52}$ (D). While the majority of bacteria did not appear to be expressing type 1 pili, piliated bacteria could be found in all four samples. Piliated bacteria displayed FimH immmunostaining at the distal tips of pili.

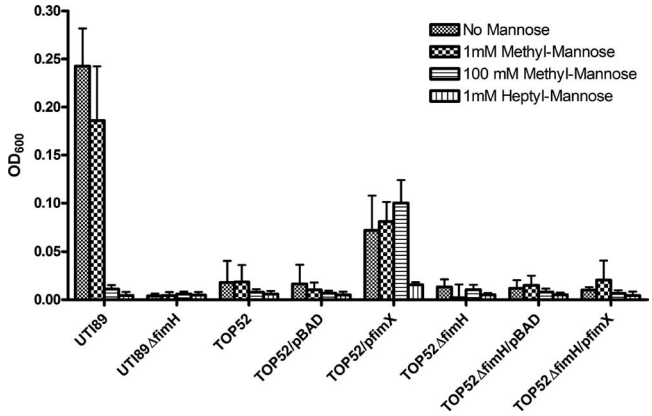

FIG. 4. Heptyl mannose, but not methyl mannose, inhibits FimH-dependent biofilm formation of *K. pneumoniae* TOP52/p*fimX*. A 48-h biofilm assay was used to quantify biofilms produced by *E. coli* UTI89 and *K. pneumoniae* TOP52 strains in the presence of no mannose, 1 mM methyl mannose, 100 mM methyl mannose, or 1 mM heptyl mannose. TOP52 forms a FimH-dependent biofilm with induced expression of type 1 pili via the *E. coli* recombinase, *fimX*. This biofilm formation is inhibited by heptyl mannose but not high concentrations of methyl mannose. UTI89 forms robust biofilm without mannose but is inhibited by heptyl mannose or high concentrations of methyl mannose. Error bars represent standard deviations.

FimH dependent. Thus, although $FimH_{52}$ is unable to mediate hemagglutination, it is capable of mediating biofilm formation. *E. coli* UTI89 formed a robust biofilm, while UTI89 Δ*fimH* did not. The formation of *E. coli* UTI89 biofilm was fully inhibited by 100 mM methyl mannose or 1 mM heptyl mannose (Fig. 4). In contrast, TOP52/p*fimX* biofilm formation was not affected by the presence of 100 mM methyl mannose, but was fully inhibited by 1 mM heptyl mannose.

Therefore, TOP52/p*fimX* forms a FimH-dependent biofilm that is inhibited by heptyl mannose but not methyl mannose. This phenotype is distinct from those of *E. coli* UTI89 FimH-dependent biofilms, which are fully inhibited by the presence of 100 mM methyl mannose.

***E. coli* UTI89 and *K. pneumoniae* TOP52 both require *fimH* for effective persistence in the urinary tract.** To analyze the respective roles of $FimH_{52}$ and $FimH_{89}$ in urinary tract infection, 10^7 CFU of *E. coli* UTI89, UTI89 Δ*fimH*, *K. pneumoniae* TOP52 or TOP52 Δ*fimH* were inoculated into the bladders of C3H/HeN mice by transurethral catheterization. Bladders and kidneys were harvested at various time points postinoculation, and bacterial titers were determined. In the bladder (Fig. 5A), *E. coli* UTI89 had significantly higher titers than UTI89 Δ*fimH* at 6 h ($P < 0.0001$), 24 h ($P < 0.0001$), and 336 h ($P = 0.0007$) postinfection. UTI89 Δ*fimH* was cleared from the bladder as time progressed. *K. pneumoniae* TOP52 had slightly but significantly higher titers ($P = 0.0244$) than TOP52 Δ*fimH* in the bladders of mice at 6 h postinoculation. By 24 h, there was no significant difference between TOP52 and TOP52 Δ*fimH* bladder titers. However, by 336 h postinfection, TOP52 Δ*fimH* had significantly lower titers than wild-type TOP52 ($P = 0.0012$). In the kidneys (Fig. 5B), UTI89 had significantly higher titers than UTI89 Δ*fimH* at 6 h postinfection ($P < 0.0001$), however the two strains had similar titers at both 24 and 336 h postinfection. TOP52 and TOP52 Δ*fimH* had similar levels of bacterial burden in the kidneys at all time points tested. Thus, FimH in *K. pneumoniae* TOP52 does not play a critical role early in bladder infection as is the case with *E. coli* UTI89; however, FimH is required for effective persistence in the bladder in both strains.

$FimH_{52}$ is required for *K. pneumoniae* TOP52 bladder invasion and IBC formation. In order to further assess the role of $FimH_{52}$ in acute *K. pneumoniae* TOP52 cystitis, bladder invasion assays were performed at 1 h postinfection with UTI89, UTI89 Δ*fimH*, TOP52, or TOP52 Δ*fimH*. In these assays, luminal bacteria were collected by successive bladder washes (Fig. 5C), prior to gentamicin treatment of the bladder to kill extracellular bacteria, as previously described (33). After 1.5 h of incubation in gentamicin, bladders were washed and homogenized and cell titers were determined to reveal the intracellular bacterial burden (Fig. 5D). UTI89 had 100-fold-higher luminal bacterial counts compared to UTI89 Δ*fimH* at 1 h postinfection ($P = 0.0043$). However, TOP52 and TOP52 Δ*fimH* had similar levels of luminal colonization. At this 1-h time point, UTI89 had significantly higher levels of intracellular bacteria than UTI89 Δ*fimH* ($P = 0.0055$), which did not have any intracellular titers above the limit of detection (5 CFU). TOP52 also invaded into the bladder tissue and had intracellular bacterial titers that were significantly higher than TOP52 Δ*fimH* ($P = 0.0095$), which did not have titers above the limit of detection.

To determine if the presence of $FimH_{52}$ affects the ability of TOP52 to form IBCs, we visualized and quantified IBCs by *lacZ* staining of whole, mounted, fixed bladders as described previously (33) at 6 h postinoculation of UTI89, UTI89 Δ*fimH*, TOP52, or TOP52 Δ*fimH* (Fig. 5E). UTI89 formed a wide range of IBCs with a median of 25.5 per bladder, while UTI89 Δ*fimH* formed no detectable IBCs. TOP52 had a median of 2.0 IBCs per bladder, while TOP52 Δ*fimH* was unable to produce detectable IBCs ($P = 0.0009$).

These data suggest that *K. pneumoniae* TOP52 $FimH_{52}$, in contrast to *E. coli* UTI89 $FimH_{89}$, does not play a significant role in early bladder colonization. However, $FimH_{52}$ is required for TOP52 invasion and IBC formation in the murine bladder, as is the case for UTI89.

***$fimH_{52}$* does not restore the ability of UTI89 Δ*fimH* to effectively infect the bladder.** *E. coli* UTI89 relies on FimH to successfully cause UTI in the murine model. The ability of $fimH_{52}$ to restore the ability of UTI89 Δ*fimH* to bind, invade, and infect murine bladders was investigated by using UTI89 Δ*fimH* complemented with pBAD vector control, p$fimH_{89}$, and p$fimH_{52}$. In 1-h gentamicin protection assays (Fig. 6A and B), UTI89 Δ*fimH* complemented with p$fimH_{89}$ had significantly higher luminal titers than the same strain complemented with vector control (Fig. 6A, $P = 0.0001$) despite the known expression deficiencies observed above. Additionally, UTI89 Δ*fimH*/p$fimH_{89}$ had significantly higher 1-h luminal titers than UTI89 Δ*fimH*/p$fimH_{52}$, which had colonization levels similar to those of the vector control. Examination of the intracellular population at 1 h (Fig. 6B) revealed that the UTI89 Δ*fimH*/pBAD vector control did not have titers above the limit of detection, whereas UTI89 Δ*fimH*/p$fimH_{89}$ did produce significantly higher burdens of intracellular bacteria ($P = 0.0028$). UTI89 Δ*fimH*/p$fimH_{52}$ was able to invade the bladder tissue, but at significantly lower levels compared to UTI89 Δ*fimH*/p$fimH_{89}$

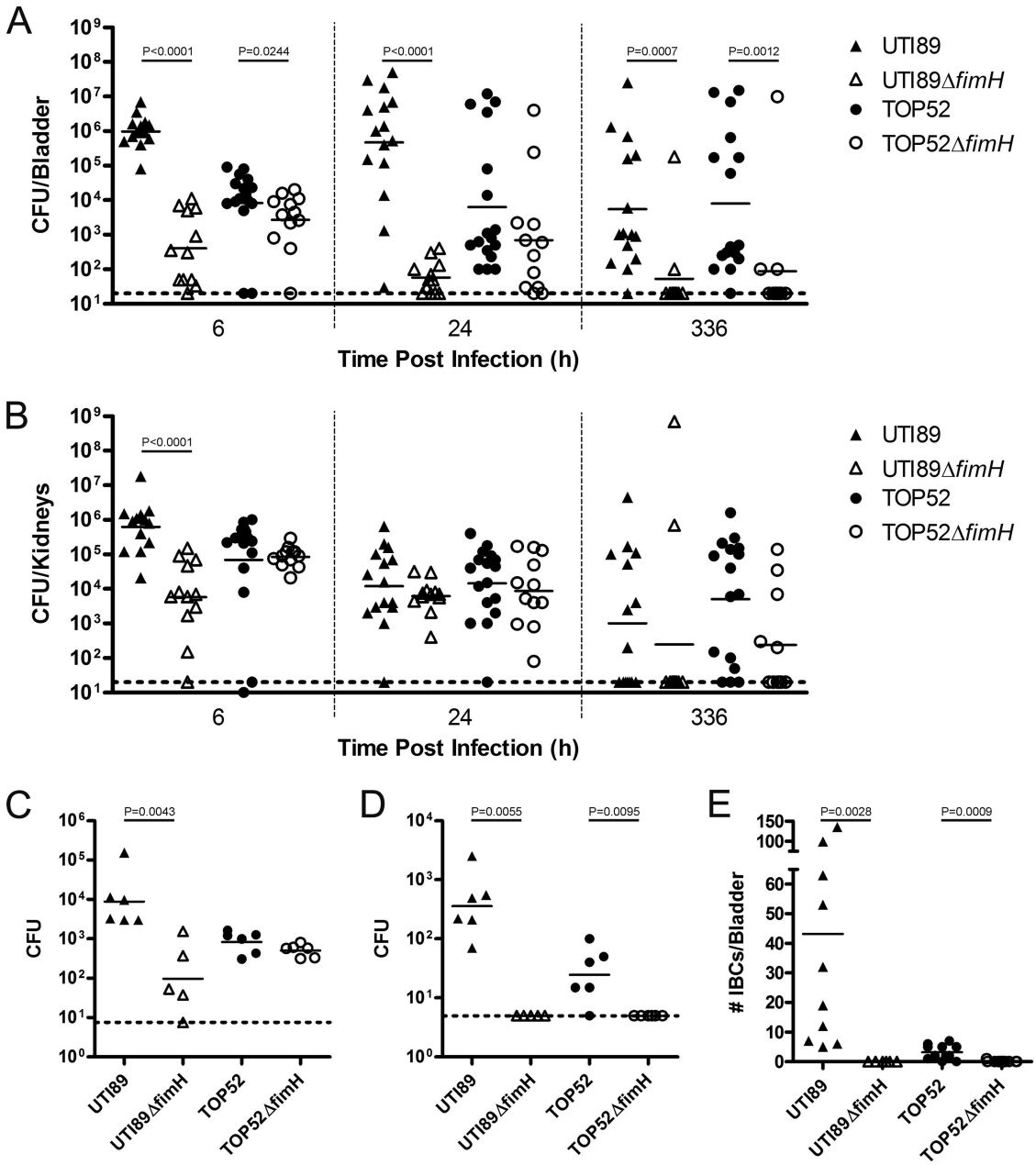

FIG. 5. FimH of *K. pneumoniae* TOP52 is required for invasion, IBC formation, and persistence but not colonization in the murine model of UTI. Female C3H/HeN mice were inoculated with 10^7 *E. coli* UTI89 (▲), UTI89 Δ*fimH* (△), *K. pneumoniae* TOP52 (●), or TOP52 Δ*fimH* (○) by transurethral inoculation. For organ titers, bladders (A) and kidneys (B) were harvested at various time points postinfection and CFU were calculated. Titer data are combined from three independent experiments. For ex vivo gentamicin protection assays, bladders were harvested at 1 h postinfection and luminal (C) and intracellular (D) populations of bacteria were quantified. IBCs were quantified (E) after visualization by LacZ staining at 6 h postinoculation. Short bars represent geometric means of each group, and horizontal dotted lines represent limits of detection. Significant *P* values, as calculated using the Mann-Whitney *U* test, are displayed.

($P = 0.0106$). At 6 h postinoculation, UTI89 Δ*fimH*/p*fimH*$_{89}$ had significantly higher burdens of bacteria in the bladder than both UTI89 Δ*fimH*/pBAD ($P = 0.0043$) and UTI89 Δ*fimH*/p*fimH*$_{52}$ ($P = 0.0032$). Complementation of UTI89 Δ*fimH* with *fimH* from either UTI89 or TOP52 did not significantly affect 6-h kidney titers compared to those of the vector control.

The *fimH*$_{52}$ gene was not able to restore UTI89 Δ*fimH* to levels above that of the vector control, while complementation with *fimH*$_{89}$ yielded higher bacterial burdens at 1 and 6 h. This suggests a potential defect in the function of FimH$_{52}$ in the bladder compared to FimH$_{89}$.

DISCUSSION

FimH of the *K. pneumoniae* strain TOP52 (FimH$_{52}$) has an amino acid sequence highly homologous to the sequence en-

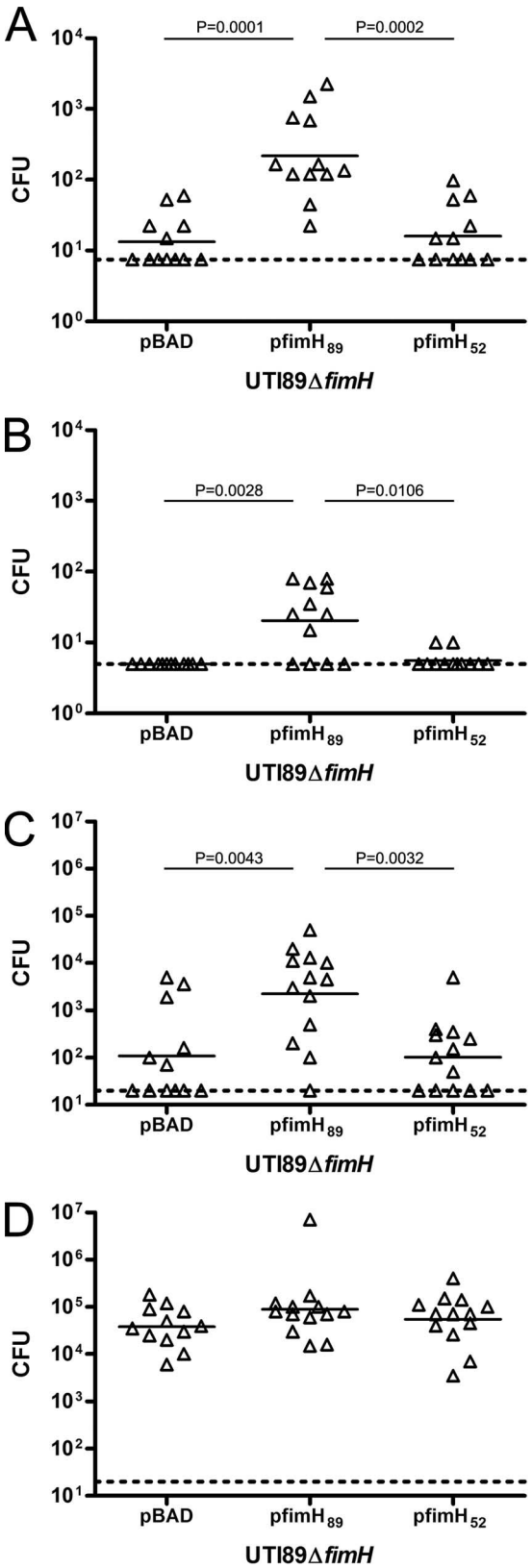

FIG. 6. Complementation of UTI89 Δ*fimH* with p*fimH*$_{89}$ but not p*fimH*$_{52}$ leads to increased bacterial burden in the murine model of UTI. Female C3H/HeN mice were inoculated with 10^7 cells of the UTI89 Δ*fimH*/pBAD vector control, UTI89 Δ*fimH*/p*fimH*$_{89}$, or UTI89 Δ*fimH*/p*fimH*$_{52}$ by transurethral inoculation. Ex vivo gentamicin protection assays were performed in which bladders were harvested at 1 h postinfection and luminal (A) and intracellular (B) populations of bacteria were quantified. For organ titers, bladders (C) and kidneys (D) were harvested at 6 h postinfection and CFU were enumerated. Short bars represent geometric means of each group, and horizontal dotted lines represent limits of detection. Significant *P* values, as calculated using the Mann-Whitney *U* test, are displayed.

coded by dozens of *fimH* genes that have been sequenced from *E. coli* (34, 54, 56). The residues that form the mannose binding pocket (Asn46, Asp47, Asp54, Gln133, Asn135, and Asp140) and hydrophobic ridge (Phe1, Ile13, Try48, Ile52, Tyr137, and Phe142) are completely identical between FimH$_{52}$ and all known FimH adhesins of *E. coli*. Despite this identity, FimH$_{52}$ has a receptor specificity unique from that of UPEC FimH. FimH$_{52}$ is unable to mediate agglutination of guinea pig erythrocytes, whereas all known UPEC FimH adhesins are defined by their ability to mediate MSHA. Different *E. coli* FimH variants have been classified as high-affinity monomannose binders or lower-affinity trimannose binders (45, 54). However, both trimannose and monomannose variants display MSHA of guinea pig erythrocytes.

E. coli FimH recognizes mannose and has been shown to be able to interact with Manα1, 3Manβ1, 4GlcNAcβ1, 4GlcNAc in an extended binding site (61). These additional interactions between FimH and extended oligomannose moieties are mimicked by butyl α-D-mannose (61). Extended alkyl-α-mannosides have higher affinities for *E. coli* FimH compared to methyl-α-D-mannopyranoside (methyl mannose), with heptyl α-D-mannopyranoside (heptyl mannose) having the lowest dissociation constant (K_d) of 5 nM (5). *K. pneumoniae* FimH-dependent biofilms could only be inhibited by heptyl mannose and not methyl mannose, arguing that *K. pneumoniae* FimH requires additional contacts of the alkyl chain outside of the mannose binding pocket.

FimH$_{52}$ differs at 17 positions from *E. coli* FimH and was threaded onto the three-dimensional structure of *E. coli* FimH. In the DE loop, adjacent to the hydrophobic ridge, Val94 and Asn96 of *E. coli* UTI89 FimH (FimH$_{89}$) are changed to Ile and Asp, respectively, in FimH$_{52}$. In the G strand, immediately C terminal to key residues in the hydrophobic ridge, Val145 in FimH$_{89}$ is changed to Ile in FimH$_{52}$. Combined, these differences may alter the structural stability of the hydrophobic ridge of FimH$_{52}$ through changes in hydrophobic and hydrogen bond contacts. Thus, although FimH$_{52}$ is unable to bind methyl mannose, these amino acid changes may facilitate interactions with longer oligomannose substrates (61).

The inability of FimH$_{52}$ to mediate hemagglutination may be due to amino acid changes in proximity to the mannose binding pocket. Gln133 and Asp140 *E. coli* FimH residues are required for HA titers and mannose binding (29). Two differences in *K. pneumoniae* TOP52 primary sequence exist in residues adjacent to these mannose-binding residues at positions 132 and 141. Data from the threaded model suggest that at least two hydrogen bonds are lost in FimH$_{52}$ with the combined differences in residues 132 and 141, which may have a destabilizing effect on interactions at the mannose site around the Asp140 and Gln133 mannose-binding resi-

dues. Sequence variation in regions of FimH not in close proximity to the mannose binding pocket may also significantly affect FimH function (56, 57).

Studies have suggested that fimbrial shafts can influence binding specificities of type 1 pili (16, 38). These effects do not account for the binding specificity differences observed for $FimH_{52}$. $FimH_{52}$ assembled into *E. coli* UTI89 type 1 pili was also hemagglutination negative, and $FimH_{89}$ assembled into *K. pneumoniae* TOP52 type 1 pili produced an MSHA titer. Thus, the major functional disparities between *E. coli* and *K. pneumoniae* type 1 pili were specific to the AD of FimH, not the strain background or fimbrial shaft. However, fimbrial shafts may influence FimH binding in more subtle ways that could have been missed in this study due to the lower expression of type 1 pili in *fimH*-knockout backgrounds.

The binding specificity differences observed for $FimH_{52}$ result in dramatic functional differences seen in *K. pneumoniae* UTI pathogenesis compared to *E. coli* UTI pathogenesis. Although *K. pneumoniae* TOP52 requires FimH for invasion and IBC formation in the murine bladder, FimH is not essential for early colonization. TOP52 and TOP52 Δ*fimH* have similar 1-h luminal bladder titers, 24-h whole-bladder titers, and only modest titer differences at 6 h postinfection. The small but significant differences at 6 h likely represent the intracellular population of bacteria in IBCs within TOP52-infected bladders that are absent in TOP52 Δ*fimH*-infected bladders. *K. pneumoniae* may use a different, non-type 1 pilus adhesin for initial binding to the bladder surface that *E. coli* lacks. This would explain why TOP52 Δ*fimH* had higher 1-h luminal titers and 6-h whole-bladder titers compared to UTI89 Δ*fimH*. *K. pneumoniae* contains a gene that encodes type 3 pili; however, these pili have not been implicated in binding to the bladder surface and are thought to mediate attachment to the basolateral surface of tracheal epithelial cells and basement membrane components (60). In addition to type 1 and type 3 pili, *K. pneumoniae* genes encode at least two other non-pilus adhesins. The CF29K and KPF-28 adhesins may play important roles in mediating attachment within the mammalian intestine, but their role in UTI has not been investigated (9, 12).

For many years, the glycoprotein uroplakin Ia has been considered the main receptor mediating FimH-dependent adhesion in the bladder (42, 63). Recently, it has been shown that host cell integrins also can mediate type 1 pilus-dependent invasion of urothelial cells (17). We currently do not know if *K. pneumoniae* $FimH_{52}$ is capable of binding these receptors. It is possible that $FimH_{52}$ may only be capable of binding integrin receptors (and not uroplakin Ia) for invasion of urothelial cells but not necessarily mediating significant adhesion to the uroplakin-coated bladder surface. Alternatively, *K. pneumoniae* FimH may have evolved for binding to a receptor in a different environment from the bladder.

This work focused on a single uropathogenic isolate of *K. pneumoniae*, and it is important to extend this work to other strains. The sequence of TOP52 FimH was almost identical to those of other sequenced *K. pneumoniae* FimH proteins and thus may be representative. The inability of *K. pneumoniae* TOP52 to agglutinate guinea pig RBCs is not an isolated finding. The ATCC 700721 strain also lacks an MSHA titer. The first studies of fimbriae and adhesive properties of 154 *K. pneumoniae* isolates found that 57.6% of strains produced little or no MSHA titer (13). Many researchers considered this to be due to poor type 1 expression in *K. pneumoniae*. However, *K. pneumoniae* TOP52 remained hemagglutination negative when expression of type 1 pili was increased by deletion of *fimK* or overexpression of *fimX*. Additionally, expression of *E. coli* type 1 pili at similar levels to TOP52 type 1 pili resulted in a positive MSHA.

This study suggests that limited sequence variation between the FimH of *E. coli* and *K. pneumoniae* results in differences in function and ability to colonize the urinary tract. Despite its poor adhesive properties in the urinary tract, FimH of *K. pneumoniae* remains an important virulence factor. It enables *K. pneumoniae* to progress through an IBC pathway during UTI and ultimately persist in the host. *K. pneumoniae* FimH likely requires ligand-receptor contacts outside of the mannose binding pocket for efficient binding. Further insight into these structural determinants will aid in our understanding of the altered host-pathogen interactions of *K. pneumoniae* UTI.

ACKNOWLEDGMENTS

We thank Stefan Oscarson for the heptyl mannose. We also thank Wandy Beatty for assistance with electron microscopy experiments, Chia Hung for help with mouse experiments, and Melissa Kraus for statistical support.

This work was supported by the National Institutes of Health, Office of Research on Women's Health: Specialized Center of Research on Sex and Gender Factors Affecting Women's Health, grant DK64540; National Institute of Diabetes and Digestive and Kidney Diseases, grant R01 DK051406; and National Institute of Allergy and Infectious Diseases, grants R01 AI29549 and R01 AI48689.

REFERENCES

1. **Anderson, G. G., J. J. Palermo, J. D. Schilling, R. Roth, J. Heuser, and S. J. Hultgren.** 2003. Intracellular bacterial biofilm-like pods in urinary tract infections. Science **301:**105–107.
2. **Bahrani-Mougeot, F. K., E. L. Buckles, C. V. Lockatell, J. R. Hebel, D. E. Johnson, C. M. Tang, and M. S. Donnenberg.** 2002. Type 1 fimbriae and extracellular polysaccharides are preeminent uropathogenic *Escherichia coli* virulence determinants in the murine urinary tract. Mol. Microbiol. **45:**1079–1093.
3. **Barnhart, M. M., F. G. Sauer, J. S. Pinkner, and S. J. Hultgren.** 2003. Chaperone-subunit-usher interactions required for donor strand exchange during bacterial pilus assembly. J. Bacteriol. **185:**2723–2730.
4. **Bennett-Lovsey, R. M., A. D. Herbert, M. J. Sternberg, and L. A. Kelley.** 2008. Exploring the extremes of sequence/structure space with ensemble fold recognition in the program Phyre. Proteins **70:**611–625.
5. **Bouckaert, J., J. Berglund, M. Schembri, E. De Genst, L. Cools, M. Wuhrer, C. S. Hung, J. Pinkner, R. Slattegard, A. Zavialov, D. Choudhury, S. Langermann, S. J. Hultgren, L. Wyns, P. Klemm, S. Oscarson, S. D. Knight, and H. De Greve.** 2005. Receptor binding studies disclose a novel class of high-affinity inhibitors of the *Escherichia coli* FimH adhesin. Mol. Microbiol. **55:**441–455.
6. **Brinton, C. C., Jr.** 1965. The structure, function, synthesis, and genetic control of bacterial pili and a model for DNA and RNA transport in Gram negative bacteria. Trans. N. Y. Acad. Sci. **27:**1003–1165.
7. **Bryan, A., P. Roesch, L. Davis, R. Moritz, S. Pellett, and R. A. Welch.** 2006. Regulation of type 1 fimbriae by unlinked FimB- and FimE-like recombinases in uropathogenic *Escherichia coli* strain CFT073. Infect. Immun. **74:**1072–1083.
8. **Choudhury, D., A. Thompson, V. Stojanoff, S. Langermann, J. Pinkner, S. J. Hultgren, and S. D. Knight.** 1999. X-ray structure of the FimC-FimH chaperone-adhesin complex from uropathogenic *Escherichia coli*. Science **285:**1061–1066.
9. **Darfeuille-Michaud, A., C. Jallat, D. Aubel, D. Sirot, C. Rich, J. Sirot, and B. Joly.** 1992. R-plasmid-encoded adhesive factor in *Klebsiella pneumoniae* strains responsible for human nosocomial infections. Infect. Immun. **60:**44–55.
10. **Datsenko, K. A., and B. L. Wanner.** 2000. One-step inactivation of chromo-

somal genes in Escherichia coli K-12 using PCR products. Proc. Natl. Acad. Sci. USA **97:**6640–6645.
11. **DeLano, W. L.** 2002. The PyMOL molecular graphics system. DeLano Scientific, Palo Alto, CA. http://www.pymol.org.
12. **Di Martino, P., V. Livrelli, D. Sirot, B. Joly, and A. Darfeuille-Michaud.** 1996. A new fimbrial antigen harbored by CAZ-5/SHV-4-producing *Klebsiella pneumoniae* strains involved in nosocomial infections. Infect. Immun. **64:**2266–2273.
13. **Duguid, J. P.** 1959. Fimbriae and adhesive properties in *Klebsiella* strains. J. Gen. Microbiol. **21:**271–286.
14. **Duguid, J. P., and D. C. Old.** 1980. Adhesive properties of *Enterobacteriacae*, p. 186–217. *In* E. H. Beachy (ed.), Bacterial adherence receptors and recognition. Chapman & Hall, London, United Kingdom.
15. **Duguid, J. P., I. W. Smith, G. Dempster, and P. N. Edmunds.** 1955. Nonflagellar filamentous appendages ("fimbriae") and hemagglutinating activity in *bacterium coli*. J. Pathol. Bacteriol. **70:**335–348.
16. **Duncan, M. J., E. L. Mann, M. S. Cohen, I. Ofek, N. Sharon, and S. N. Abraham.** 2005. The distinct binding specificities exhibited by enterobacterial type 1 fimbriae are determined by their fimbrial shafts. J. Biol. Chem. **280:**37707–37716.
17. **Eto, D. S., T. A. Jones, J. L. Sundsbak, and M. A. Mulvey.** 2007. Integrin-mediated host cell invasion by type 1-piliated uropathogenic *Escherichia coli*. PLoS Pathog. **3:**e100.
18. **Fader, R. C., and C. P. Davis.** 1980. Effect of piliation on *Klebsiella pneumoniae* infection in rat bladders. Infect. Immun. **30:**554–561.
19. **Firon, N., S. Ashkenazi, D. Mirelman, I. Ofek, and N. Sharon.** 1987. Aromatic alpha-glycosides of mannose are powerful inhibitors of the adherence of type 1 fimbriated *Escherichia coli* to yeast and intestinal epithelial cells. Infect. Immun. **55:**472–476.
20. **Firon, N., I. Ofek, and N. Sharon.** 1984. Carbohydrate-binding sites of the mannose-specific fimbrial lectins of enterobacteria. Infect. Immun. **43:**1088–1090.
21. **Firon, N., I. Ofek, and N. Sharon.** 1983. Carbohydrate specificity of the surface lectins of *Escherichia coli*, *Klebsiella pneumoniae* and *Salmonella typhimurium*. Carbohydr. Res. **120:**235–249.
22. **Garofalo, C. K., T. M. Hooton, S. M. Martin, W. E. Stamm, J. J. Palermo, J. I. Gordon, and S. J. Hultgren.** 2007. *Escherichia coli* from urine of female patients with urinary tract infections is competent for intracellular bacterial community formation. Infect. Immun. **75:**52–60.
23. **Gerlach, G.-F., S. Clegg, and B. L. Allen.** 1989. Identification and characterization of the genes encoding the type 3 and type 1 fimbrial adhesins of *Klebsiella pneumoniae*. J. Bacteriol. **171:**1262–1270.
24. **Guzman, L.-M., D. Belin, M. J. Carson, and J. Beckwith.** 1995. Tight regulation, modulation, and high-level expression by vectors containing the arabinose P_{BAD} promoter. J. Bacteriol. **177:**4121–4130.
25. **Hannan, T. J., I. U. Mysorekar, S. L. Chen, J. N. Walker, J. M. Jones, J. S. Pinkner, S. J. Hultgren, and P. C. Seed.** 2007. LeuX tRNA-dependent and -independent mechanisms of *Escherichia coli* pathogenesis in acute cystitis. Mol. Microbiol. **67:**116–128.
26. **Hull, R. A., R. E. Gill, P. Hsu, B. H. Minshew, and S. Falkow.** 1981. Construction and expression of recombinant plasmids encoding type 1 or D-mannose-resistant pili from a urinary tract infection *Escherichia coli* isolate. Infect. Immun. **33:**933–938.
27. **Hultgren, S. J., T. N. Porter, A. J. Schaeffer, and J. L. Duncan.** 1985. Role of type 1 pili and effects of phase variation on lower urinary tract infections produced by *Escherichia coli*. Infect. Immun. **50:**370–377.
28. **Hultgren, S. J., W. R. Schwan, A. J. Schaeffer, and J. L. Duncan.** 1986. Regulation of production of type 1 pili among urinary tract isolates of *Escherichia coli*. Infect. Immun. **54:**613–620.
29. **Hung, C.-S., J. Bouckaert, D. Hung, J. Pinkner, C. Widberg, A. De Fusco, C. G. Auguste, B. Strouse, S. Langerman, G. Waksman, and S. J. Hultgren.** 2002. Structure basis of tropism of *Escherichia coli* to the bladder during urinary tract infection. Mol. Microbiol. **44:**903–915.
30. **Hung, D. L., and S. J. Hultgren.** 1998. Pilus biogenesis via the chaperone/usher pathway: an integration of structure and function. J. Struct. Biol. **124:**201–220.
31. **Jones, C. H., J. S. Pinkner, R. Roth, J. Heuser, A. V. Nicholes, S. N. Abraham, and S. J. Hultgren.** 1995. FimH adhesin of type 1 pili is assembled into a fibrillar tip structure in the *Enterobacteriaceae*. Proc. Natl. Acad. Sci. USA **92:**2081–2085.
32. **Justice, S. S., C. Hung, J. A. Theriot, D. A. Fletcher, G. G. Anderson, M. J. Footer, and S. J. Hultgren.** 2004. Differentiation and developmental pathways of uropathogenic *Escherichia coli* in urinary tract pathogenesis. Proc. Natl. Acad. Sci. USA **101:**1333–1338.
33. **Justice, S. S., S. R. Lauer, S. J. Hultgren, and D. A. Hunstad.** 2006. Maturation of intracellular *Escherichia coli* communities requires SurA. Infect. Immun. **74:**4793–4800.
34. **Klemm, P., and G. Christiansen.** 1987. Three *fim* genes required for the regulation of length and mediation of adhesion of *Escherichia coli* type 1 fimbriae. Mol. Gen. Genet. **208:**439–445.
35. **Langermann, S., R. Mollby, J. E. Burlein, S. R. Palaszynski, C. G. Auguste, A. DeFusco, R. Strouse, M. A. Schenerman, S. J. Hultgren, J. S. Pinkner, J. Winberg, L. Guldevall, M. Soderhall, K. Ishikawa, S. Normark, and S. Koenig.** 2000. Vaccination with FimH adhesin protects cynomolgus monkeys from colonization and infection by uropathogenic *Escherichia coli*. J. Infect. Dis. **181:**774–778.
36. **Langermann, S., S. Palaszynski, M. Barnhart, G. Auguste, J. S. Pinkner, J. Burlein, P. Barren, S. Koenig, S. Leath, C. H. Jones, and S. J. Hultgren.** 1997. Prevention of mucosal *Escherichia coli* infection by FimH-adhesin-based systemic vaccination. Science **276:**607–611.
37. **Link, A. J., D. Phillips, and G. M. Church.** 1997. Methods for generating precise deletions and insertions in the genome of wild-type *Escherichia coli*: application to open reading frame characterization. J. Bacteriol. **179:**6228–6237.
38. **Madison, B., I. Ofek, S. Clegg, and S. N. Abraham.** 1994. Type 1 fimbrial shafts of *Escherichia coli* and *Klebsiella pneumoniae* influence sugar-binding specificities of their FimH adhesins. Infect. Immun. **62:**843–848.
39. **Martinez, J. J., M. A. Mulvey, J. D. Schilling, J. S. Pinkner, and S. J. Hultgren.** 2000. Type 1 pilus-mediated bacterial invasion of bladder epithelial cells. EMBO J. **19:**2803–2812.
40. **Matatov, R., J. Goldhar, E. Skutelsky, I. Sechter, R. Perry, R. Podschun, H. Sahly, K. Thankavel, S. N. Abraham, and I. Ofek.** 1999. Inability of encapsulated *Klebsiella pneumoniae* to assemble functional type 1 fimbriae on their surface. FEMS Microbiol. Lett. **179:**123–130.
41. **McClelland, M., L. Florea, K. Sanderson, S. W. Clifton, J. Parkhill, C. Churcher, G. Dougan, R. K. Wilson, and W. Miller.** 2000. Comparison of the *Escherichia coli* K-12 genome with sampled genomes of a *Klebsiella pneumoniae* and three *Salmonella enterica* serovars, Typhimurium, Typhi, and Paratyphi. Nucleic Acids Res. **28:**4974–4986.
42. **Mulvey, M. A., Y. S. Lopez-Boado, C. L. Wilson, R. Roth, W. C. Parks, J. Heuser, and S. J. Hultgren.** 1998. Induction and evasion of host defenses by type 1-piliated uropathogenic *Escherichia coli*. Science **282:**1494–1497.
43. **Mulvey, M. A., J. D. Schilling, and S. J. Hultgren.** 2001. Establishment of a persistent *Escherichia coli* reservoir during the acute phase of a bladder infection. Infect. Immun. **69:**4572–4579.
44. **Murphy, K. C., and K. G. Campellone.** 2003. Lambda Red-mediated recombinogenic engineering of enterohemorrhagic and enteropathogenic *E. coli*. BMC Mol. Biol. **4:**11.
45. **Nilsson, L. M., W. E. Thomas, E. Trintchina, V. Vogel, and E. V. Sokurenko.** 2006. Catch bond-mediated adhesion without a shear threshold: trimannose versus monomannose interactions with the FimH adhesin of *Escherichia coli*. J. Biol. Chem. **281:**16656–16663.
46. **O'Toole, G. A., and R. Kolter.** 1998. Initiation of biofilm formation in *Pseudomonas fluorescens* WCS365 proceeds via multiple, convergent signalling pathways: a genetic analysis. Mol. Microbiol. **28:**449–461.
47. **Ottow, J. C. G.** 1975. Ecology, physiology and genetics of fimbriae and pili. Annu. Rev. Microbiol. **29:**79.
48. **Ronald, A. R., L. E. Nicolle, E. Stamm, J. Krieger, J. Warren, A. Schaeffer, K. G. Naber, T. M. Hooton, J. Johnson, S. Chambers, and V. Andriole.** 2001. Urinary tract infection in adults: research priorities and strategies. Int. J. Antimicrob. Agents **17:**343–348.
49. **Ronald, A. R., and A. L. Pattullo.** 1991. The natural history of urinary infection in adults. Med. Clin. N. Am. **75:**299–312.
50. **Rosen, D. A., J. S. Pinkner, J. M. Jones, J. N. Walker, S. Clegg, and S. J. Hultgren.** 2008. Utilization of an intracellular bacterial community pathway in *Klebsiella pneumoniae* urinary tract infection and the effects of FimK on type 1 pilus expression. Infect. Immun. **76:**3337–3345.
51. **Rosen, D. A., T. M. Hooton, W. E. Stamm, P. A. Humphrey, and S. J. Hultgren.** 2007. Detection of intracellular bacterial communities in human urinary tract infection. PLoS Med. **4:**e329.
52. **Salit, I. E., and E. C. Gotschlich.** 1977. Hemagglutination by purified type 1 *Escherichia coli* pili. J. Exp. Med. **146:**1169–1181.
53. **Saulino, E. T., D. G. Thanassi, J. S. Pinkner, and S. J. Hultgren.** 1998. Ramifications of kinetic partitioning on usher-mediated pilus biogenesis. EMBO J. **17:**2177–2185.
54. **Sokurenko, E. V., V. Chesnokova, R. J. Doyle, and D. L. Hasty.** 1997. Diversity of the *Escherichia coli* type 1 fimbrial lectin. Differential binding to mannosides and uroepithelial cells. J. Biol. Chem. **272:**17880–17886.
55. **Sokurenko, E. V., H. S. Courtney, S. N. Abraham, P. Klemm, and D. L. Hasty.** 1992. Functional heterogeneity of type 1 fimbriae of *Escherichia coli*. Infect. Immun. **60:**4709–4719.
56. **Sokurenko, E. V., H. S. Courtney, J. Maslow, A. Siitonen, and D. L. Hasty.** 1995. Quantitative differences in adhesiveness of type 1 fimbriated *Escherichia coli* due to structural differences in *fimH* genes. J. Bacteriol. **177:**3680–3686.
57. **Sokurenko, E. V., H. S. Courtney, D. E. Ohman, P. Klemm, and D. L. Hasty.** 1994. FimH family of type 1 fimbrial adhesins: functional heterogeneity due to minor sequence variations among *fimH* genes. J. Bacteriol. **176:**748–755.
58. **Struve, C., and K. A. Krogfelt.** 1999. In vivo detection of *Escherichia coli* type 1 fimbrial expression and phase variation during experimental urinary tract infection. Microbiology **145:**2683–2690.
59. **Svanborg Eden, C., L. Hagberg, L. A. Hanson, S. Hull, R. Hull, U. Jodal, H.**

Leffler, H. Lomberg, and E. Straube. 1983. Bacterial adherence—a pathogenetic mechanism in urinary tract infections caused by *Escherichia coli*. Prog. Allergy **33:**175–188.

60. **Tarkkanen, A. M., B. L. Allen, B. Westerlund, H. Holthofer, P. Kuusela, L. Risteli, S. Clegg, and T. K. Korhonen.** 1990. Type V collagen as the target for type-3 fimbriae, enterobacterial adherence organelles. Mol. Microbiol. **4:**1353–1361.
61. **Wellens, A., C. Garofalo, H. Nguyen, N. Van Gerven, R. Slättegård, J. P. Hernalsteens, L. Wyns, S. Oscarson, H. De Greve, S. J. Hultgren, and J. Bouckaert.** 2008. Intervening with urinary tract infections using anti-adhesives based on the crystal structure of the FimH-oligomannose-3 complex. PLoS One **3**:e2040.
62. **Wright, K. J., P. C. Seed, and S. J. Hultgren.** 2007. Development of intracellular bacterial communities of uropathogenic *Escherichia coli* depends on type 1 pili. Cell. Microbiol. **9:**2230–2241.
63. **Wu, X. R., T. T. Sun, and J. J. Medina.** 1996. In vitro binding of type 1-fimbriated *Escherichia coli* to uroplakins Ia and Ib: relation to urinary tract infections. Proc. Natl. Acad. Sci. USA **93:**9630–9635.

Editor: A. J. Bäumler